



ENHANCING LIVER DISEASE DIAGNOSIS THROUGH TEXTURE-BASED CLASSIFICATION OF CT IMAGES: A COMPUTER-AIDED DIAGNOSTIC APPROACH

Fatima Hussain¹, Mehrun Nisa^{2*}, Marina Riasat³, Wajeha Shafqat⁴, Nimra Batool⁵, Faheem Afzal⁶, Aalia Nazir⁷, Ambreen Kalsoom⁸

^{1,2*,3,4,5,8}Department of Physics, The Government Sadiq College Women University Bahawalpur, Punjab – Pakistan.

⁶Associate Professor, PSRD College of Rehabilitation Sciences, Lahore - Pakistan

⁷Institute of Physics, The Islamia University of Bahawalpur - Pakistan

***Corresponding Author:** Mehrun Nisa

*Department of Physics, The Government Sadiq College Women University Bahawalpur, Punjab – Pakistan.

Abstract

Background: The incident of liver diseases among patients has been consistently increasing. Early detection and precise differentiation between benign and metastasis liver tumours could potentially lead to enhance the success rate. Computed tomography imaging serves as a practical medical imaging method for evaluating liver tumours.

Objective: The primary aim of this study is to classify liver CT images using texture features, with the goal of assessing the effectiveness of a computer-aided diagnostic system for detection of liver diseases.

Methods: The dataset used in this study comprises 162 cases of benign liver conditions and 128 cases of metastatic liver conditions. Statistical texture analysis techniques, such as Gray level run length matrix, and Co-occurrence matrix are employed to extract the texture features parameters from each region of interest. A normalization approach of $\mu \pm 3\sigma$ is applied during this process to analyze the results, the Artificial Neural Network (ANN) classification method is utilized on Principal Component Analysis (PCA), Linear Discrimination Analysis (LDA) and Non- Linear Discrimination Analysis (NDA) techniques.

Results: The images are subjected to analysis using the analysis option available in MaZda software. By applying statistical features such as run length and gray level histogram, with normalization $\mu \pm 3\sigma$, the best results are obtained. This approach highlights the distinct difference between benign and metastasis liver diseases

Key words: Texture analysis, CT images, MaZda, PCA, LDA, NDA, POE+ACC.

1.Introduction

Human liver is basically a complex, 3D organ.[1] It is the second[2] largest organ of human body[3]. The liver plays vital roles in human, performing various important functions body. Its

primary function is the remarkable ability to repair itself after injury, which helps maintains the body's homeostasis and ensure the survival rate of individual. Additionally, the liver is responsible for detoxification and regulation of the body's metabolism. Inaccurate performances of these tasks by liver can lead to damage and potentially result in liver failure, which can cause significant health problems[4]. Autophagy dysfunction in both parenchymal and non-parenchymal cells of the liver can contribute to various liver disorders[5]. The prevalence of liver illness has been steadily increasing[6], leading to growing number of patients affected. Globally , liver disease is responsible for causing approximate 2 million deaths annually[7].

Liver diseases can compass both benign and cancerous conditions. Benign liver diseases include including Hepatic adenoma, Cysts[8], Focal liver lesions and Benign focal lesion[9], which are noncancerous in nature. On the other hand metastatic liver diseases consists of cancerous diseases such as Cholangiocarcinoma and Hepatocellular carcinoma[8].

Texture analysis methods have emerged as promising imaging biomarkers for diagnosis of various diseases, including colorectal cancer, esophageal cancer, and hepatic metastasis etc. These methods enable health care professional to access the response of a particular disease to treatment, providing valuable insights into effectiveness of therapeutic intervention[10]. Texture analysis involves evaluating the spatial interrelations of gray levels[11] in an image and extracting texture feature to analyze specific variation between pixel values, particularly in CT scans[12]. Texture analysis provides potentially the relevant data by calculating various texture features using pixel's signal intensity in each ROI[13]. It enhances the detection capacities and allows for the discoveries of new insight into image characteristics[14]. on the basis of texture which is a feature commonly used for this[8].

There are different methods of texture analysis that employ various computational procedures. These methods includes Statistical, Structural, and spectral techniques[15] such as transform, fractal dimensions, structural, or spectral techniques such as transforms, Fractal dimensions, statistical moments, auto covariance, co-occurrence matrices, run-length matrices, and spectral measures are commonly used to express texture[8]. Machine vision techniques and processing of medical images have proven to be successful and advantageous for the analysis of medical images. statistical methods are often employed to analyze images [16]. And the software program MaZda is specifically used for texture of 2D images. MaZda provides comprehensive approach to quantitatively analyze the texture of image, including texture feature calculation, texture extraction, and texture segmentation[17].

2. Methods and Materials

2.1 Experimental Data

CT images of the liver were used as experimental data, and machine learning methods were applied to classify benign and metastatic liver diseases. A total of 162 CT images of benign (primary) liver conditions and 128 metastatic liver conditions were included in the study. Additionally, 20 CT images of normal livers were included to serve as a basis for comparison with the diseased liver with the normal liver. These CT images were obtained through collaboration of Diagnostic Imaging and Radiology department of Bahawalpur Victoria Hospital and Civil Hospital Bahawalpur. For texture analysis, the CT images of each patient were loaded in MaZda software.

2.2 Imaging Technique

Since the 19th century, imaging techniques have been used as important elements in biological imaging that don not hurt and provide the information about the inner parts of the body. Among these techniques, Computed Tomography scan plays a significant role in better diagnosis and treatment of many diseases, including liver diseases. Ct scan utilizes multiple x-rays (ionizing radiation) to depict the body layer-by-layer. To establish a final diagnosis, the gold standard

involves using Serum alpha-fetoprotein (AFP) and a triphasic multidetector CT scan of the liver, which employs non-ionic intravenous (IV) ultravist contrast to highlight pathological patterns. These images are obtained using a 128-slice scanner with a 12-bit depth. The thickness of the slice varies typically ranges from approximately 0.6 to 1 mm.

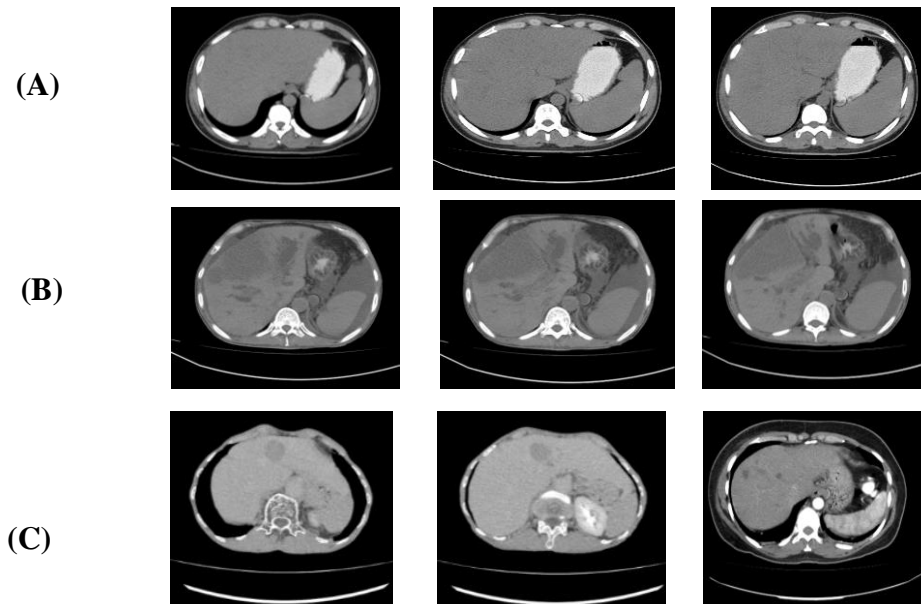


Figure 1: CT images of (A) Normal liver (B) Primary diseased liver (C) Metastatic diseased liver

2.3 Regions of Interest (RIOs)

For texture analysis, the MaZda software is utilized and all the images are in BMP format to ensure the compatibility with MaZda. CT images exhibit various structural components that appear distinct on the basis of different intensity values. Computational work focuses on exploring and analyzing these different components. Those components play a significant role and are directly related to the analysis. In the case of two dimensional CT images, the different groups of pixels are referred to region of interest. In three dimensional, these groups are called voxels. ROIs hold significant importance in the analysis of biomedical images. In this study, skilled radiologists have marked region of interest with their consent. Determining the appropriate size of region of interest from the diseased area is important for accurately identifying and characterizing texture features.

2.4 Features Extraction

Feature extraction refers to the process of converting an image into set of features that capture important features and characteristics of an image. In this research work focused on the classification of different liver diseases, the approach is based on the extracting information about pixels of the images to derive insights and features that can aid in classification task. Statistical analysis plays an important role in extracting meaningful characteristics that effectively describe the texture. This approach allows a more flexible and data driven analysis, that can be used for various purposes such as machine learning and image processing.

2.4.1 Histogram-Based Features

The quantitative information of an image is obtained through the use of a histogram. The histogram provides the distribution of intensity level within the image and this information can be used to derive various features. One such feature is probability density of occurrence for each intensity level, which is obtained by dividing the histogram values of an intensity level by the total number of pixels in an image

$$P(i) = h(i)/NM, i=0,1,..G-1$$

N represents the number of the resolved cells in the spatial domain horizontally, while M represents the number of resolved cells in spatial domain vertically. G refers to the total number of the gray level of an image. Following are the histogram-based features:

$$\begin{aligned} \text{Mean:} \quad \mu &= \sum_{l=1}^{G-1} lp(i) \\ \text{Variance:} \quad \sigma^2 &= \sum_{l=1}^{G-1} (l - \mu)^2 p(i) \\ \text{Skewness:} \quad \mu_3 &= \sigma^{-3} \sum_{l=1}^{G-1} (l - \mu)^3 p(i) \\ \text{Kurtosis:} \quad \mu_4 &= \sum_{l=1}^{G-1} [lp(i)]^2 \end{aligned}$$

2.4.2 Gradient-Based Parameters

The absolute gradient value is calculated for each pixel as a part of gradient based parameters. These parameters are derived from analyzing the changes in the intensity values across neighboring pixels. Here are some commonly used gradient based parameters:

$$\begin{aligned} \text{Mean absolute gradient:} \quad GrMean &= \frac{1}{M} \sum_{ij \in ROI} ABSV(i, j) \\ \text{Variance of absolute gradient:} \quad GrVariance &= \frac{1}{M} \sum_{ij \in ROI} (ABSV(i, j) - GrMean)^2 \\ \text{Skewness of absolute gradient:} \end{aligned}$$

$$GrSkewness = \frac{1}{(\sqrt{GrVariance})^3} \frac{1}{M} \sum_{ij \in ROI} (ABSV(i, j) - GrMean)^3$$

Kurtosis of absolute gradient:

$$GrKurtosis = \frac{1}{(\sqrt{GrVariance})^4} \frac{1}{M} \sum_{ij \in ROI} (ABSV(i, j) - GrMean)^4 - 3$$

2.4.3 Run Length Matrix-Based Parameters

Run length based parameters are derived from analyzing the length of consecutive pixels with similar intensity values in an image. These parameters provide information about texture and spatial distribution of different intensity levels. Here is some common Run length based parameters

$$\begin{aligned} \text{Short run highlights inverse moments:} \quad ShrtREmph &= (\sum_{i=1}^{N_e} \sum_{j=1}^{N_r} \frac{p(i, j)}{j^2}) / C \\ \text{Long run highlights moments:} \quad LngREmph &= (\sum_{i=1}^{N_e} \sum_{j=1}^{N_r} j^2 p(i, j)) / C \\ \text{Grey level non-uniformity:} \quad GLenNonUni &= (\sum_{i=1}^{N_e} (\sum_{j=1}^{N_r} p(i, j))^2) / C \\ \text{Run length non-uniformity:} \quad RLNonUni &= (\sum_{i=1}^{N_e} (\sum_{j=1}^{N_r} p(i, j))^2) / C \\ \text{Fraction of image in runs:} \quad Fraction &= \sum_{i=1}^{N_e} \sum_{j=1}^{N_r} p(i, j) / \sum_{i=1}^{N_e} \sum_{j=1}^{N_r} jp(i, j) \end{aligned}$$

Where the coefficient C is;

$$C = \sum_{i=1}^{N_e} \sum_{j=1}^{N_r} p(i, j)$$

These Run length matrix-based parameters are measured in four directions: in Vertical direction (Vertl-), Horizontal direction (Hozl-), biased at 45⁰ and biased at 135⁰.

2.4.4 Co-occurrence Matrix-Derived Parameters

The introduction of second order histogram features such as Co-occurrence matrix Haralic features allows for detailed analysis of image's texture and spatial relationship. These features consider the occurrences and statistical means of the intensity values within specific neighborhood distances and angles.

$$\text{Angular second moment:} \quad AngScMom = \sum_{i=1}^{N_e} \sum_{j=1}^{N_r} p(i, j)^2$$

Contrast:	$Contrast = \sum_{\pi=0}^{N_g} n^2 \sum_{i=1}^{N_e} \sum_{j=1}^{N_r} p(i, j)$
Correlation:	$Correlat = \sum_{i=1}^{N_g} \sum_{j=1}^{N_g} ij p(i, j) - \mu_x \mu_y / \rho_x \rho_y$
Sum of squares:	$SumOFSqs = \sum_{i=1}^{N_g} \sum_{j=1}^{N_g} (i - \mu_x)^2 p(i, j)$
Sum average:	$SumAverg = \sum_{i=1}^{2N_g} iP_{x+y}(i)$
Sum variance:	$SumVarnc = \sum_{i=1}^{2N_g} (i - SumAverg)^2 p_{x+y}(i)$
Sum entropy:	$SumEntrp = - \sum_{i=1}^{2N_g} p_{x+y}(i) \log(p_{x+y}(i))$
Entropy:	$Entropy = \sum_{i=1}^{N_g} \sum_{j=1}^{N_g} p(i, j) \log(p(i, j))$
Difference entropy	$DifEntrp = - \sum_{i=1}^{N_g} p_{x-y} \log(p_{x-y}(i))$

2.4.5 Autoregressive Model Parameters

In the autoregressive (AR) model, it is supposed or assumed that there exists a local interaction among the pixels of image in terms of pixel intensity. This interaction is modeled as a weighted sum of intensities of pixels in neighborhood of a specific pixel. For an image f which is considered as a zero-mean random field, an Autoregressive model can be defined as follows

$$f_s = \sum_{r \in N_s} \theta_r f_r + e_s$$

Overall the autoregressive model describe how each pixel in an image canbe estimated based on the intensities of its neighbouring pixels, with the weight defined by the parameters θ .

2.5 Features Selection

In texture analysis numerous statistical texture parameters are computed for each region of interest. However, not all of these parameters are significant for performing texture analysis. Therefore it becomes necessary to select the relevant parameters that contribute the most to the analysis. Manual selection process can be a challenging task, so various methods are employed for automated feature selection. These methods are chosen based on several properties such as data type, data size and data quality which eliminating unnecessary features. Among the different methods three basic methods are commonly used; In this research we have adopted POE+ACC feature selection method using MaZda software for selection and analysis of these features.

- POE+ACC (Probability of error and average correlation co-efficient) focuses on minimizing both the classification error probability (POE) and average correlation coefficients (ACC) between selected features to enhance the accuracy and effectiveness of classification.

$$f = f_j: \min_j [POE (f_j)]$$

$$POE (f_j) = \frac{\text{number of samples not properly classified, marked in block}}{\text{total number of samples}}$$

2.6 Feature Reduction

MaZda helps in minimizing the dimensions of features by apply various techniques, one such technique is

- **PCA (Principal Component Analysis) also known as** Karhunen-Loeve Transform (KLT). PCA reduces the dimensionality of feature data while retaining essential information. This process id referred to as parsimonious summarization.

From linear transform X to Y PCA of a given set of data can be measured if:

$$Y = P^t (X - \mu) \rightarrow Y_i = Y_{(i)}^t (X - \mu)$$

- **LDA (Liner discriminant analysis):** Secondly MaZda software enhances the discriminative power of features by applying vector transformation LDA is one such method used which is also known as class-based KLT and Fisher discriminate analysis. Then LDA transformation can be represented as:

$$X \rightarrow Y = \phi^t (X - \mu)$$

- **NDA (Non-linear discriminant analysis):** Additionally, NDA is another method utilizes statistical analysis. NDA involves applying a nonlinear data transformation, followed by the application of linear classifier on the transformed feature data.

2.7 Pattern Classification

After feature selection process, the next step in texture analysis of CT images is classification. In this step each pixel in an image is assigned to a specific class. In the presented there are two types of classes primary and secondary. Here artificial neural network (ANN) is utilized as tissue classifier. An ANN consists of interconnected nodes or neurons organized in layers, with each neuron performing computations on the input data and pass the result to the next layer. The output of the ANN classifier is probability map that provides valuable information about the potential presence of disease in different regions of the images. Overall the combination of feature selection and an ANN classifier allows for accurate classification of images by providing informative output for further analysis and clinical decision making. The summary of the proposed work is presented in the form of block diagram.

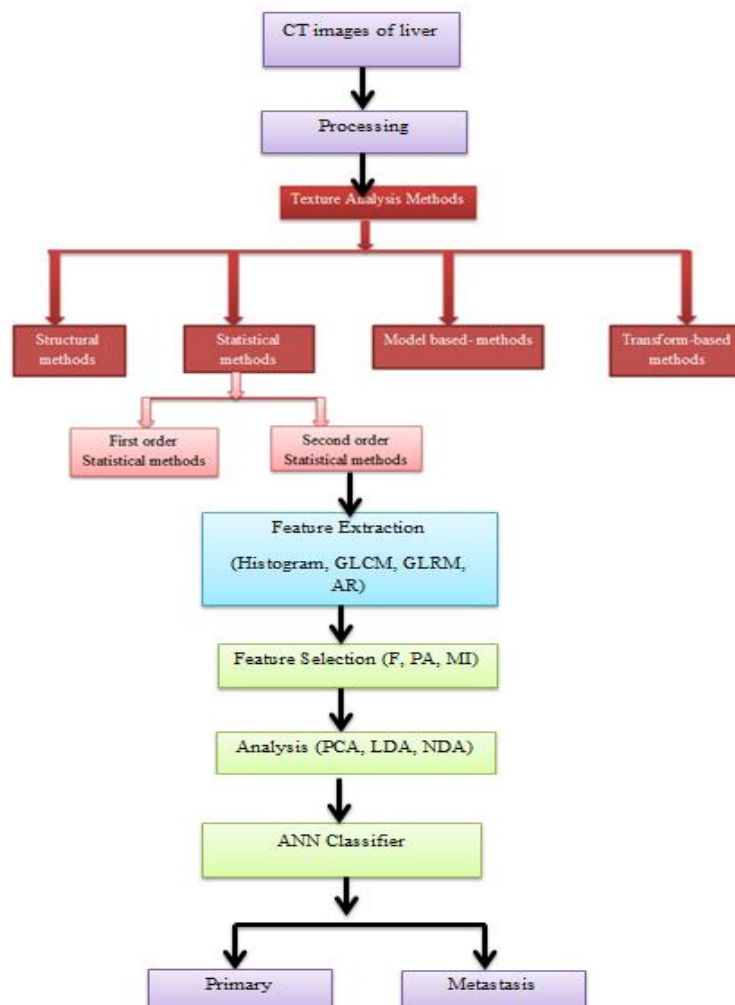


Figure 2: Block diagram of proposed work

3. Results and Discussion

The primary objective of this research is to determine the optimal conditions for the proposed technique's performance. Mazda incorporates a range of classification, visualization, and segmentation methods, along with techniques for evaluating, selecting, and extracting highly discriminative texture features [18]. Regions of interest are defined, followed by the selection of Histogram and AR model as analysis options. Texture parameters, including run-length matrix features, percentile gray values from the histogram, and measures like Sum of squares and difference entropy from the co-occurrence matrix, are extracted[19]. Prior to feature extraction, a normalization condition of $\mu \pm 3\sigma$ is applied using the POE+ACC approach. Three classification methods, PCA, LDA, and NDA, are employed, with NDA yielding the best results[20].

Feature name	1	2	3	4	5	6	7	8	9	10	11	12
Area	225	168	0	0	0	0	0	0	0	0	0	0
MinNorm	114	109	0	0	0	0	0	0	0	0	0	0
MaxNorm	146	149	0	0	0	0	0	0	0	0	0	0
Mean	130.5	129.6	0	0	0	0	0	0	0	0	0	0
Variance	28.686	44.812	0	0	0	0	0	0	0	0	0	0
Skewness	-0.054909	-0.28369	0	0	0	0	0	0	0	0	0	0
Kurtosis	-0.27412	-0.11509	0	0	0	0	0	0	0	0	0	0
Perc.01%	119	114	0	0	0	0	0	0	0	0	0	0
Perc.10%	123	120	0	0	0	0	0	0	0	0	0	0
Perc.50%	130	130	0	0	0	0	0	0	0	0	0	0
Perc.90%	137	138	0	0	0	0	0	0	0	0	0	0
Perc.99%	142	146	0	0	0	0	0	0	0	0	0	0
Area_S(1,0)	420	312	0	0	0	0	0	0	0	0	0	0
S(1,0)AngScMom	0.0064966	0.0073759	0	0	0	0	0	0	0	0	0	0
S(1,0)Contrast	103.18	81.295	0	0	0	0	0	0	0	0	0	0
S(1,0)Correlat	0.52613	0.63034	0	0	0	0	0	0	0	0	0	0
S(1,0)SumOfSqs	108.87	109.96	0	0	0	0	0	0	0	0	0	0
S(1,0)InvDiMom	0.14949	0.14139	0	0	0	0	0	0	0	0	0	0
S(1,0)SumAverg	63.19	63.91	0	0	0	0	0	0	0	0	0	0
S(1,0)SumEntrop	222.2	259.54	0	0	0	0	0	0	0	0	0	0

Figure 3: Feature Selection in MaZda

Feature name:	P:
135dr_GLevNonU	0.0000
Vertl_RLNonUni	0.0292
45dgr_GLevNonU	0.1756
135dr_RLNonUni	0.1915
45dgr_RLNonUni	0.2065
S(0,2)DifEntrp	0.2234
Vertl_GLevNonU	0.2286
S(1,1)AngScMom	0.2306
Horzl_GLevNonU	0.2336
S(2,-2)SumOfSqs	0.2379

Figure 4: POE+ACC Features Selected by MaZda Software

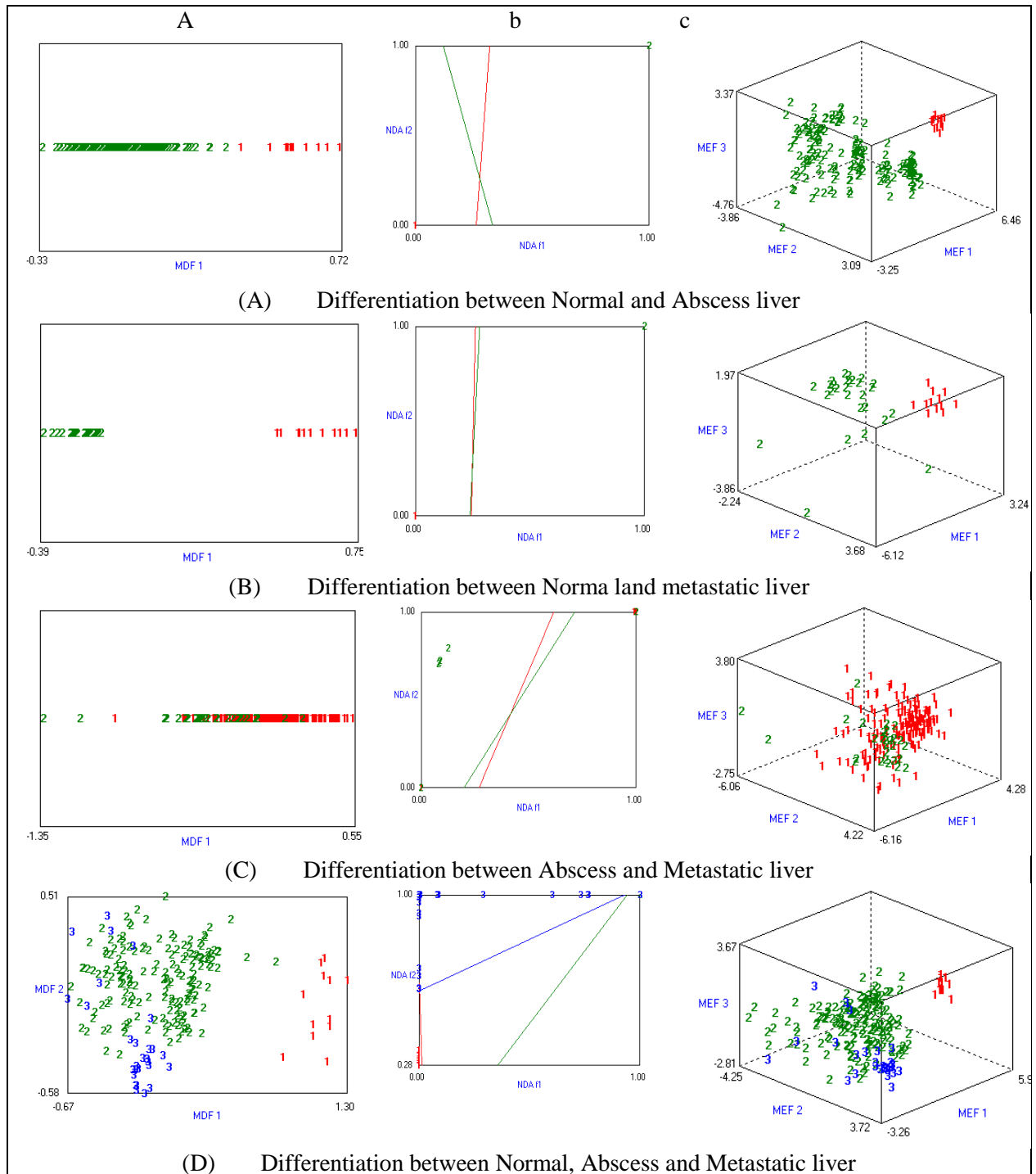


Figure 5: Comparison graphs of (a) LDA (b) NDA (c) PCA between (A) Normal liver and abscess liver. (B) Normal liver and metastasis liver (C) Abscess liver and metastasis liver. (D) Normal liver, Abscess liver and Metastatic liver.

The output of the analysis is presented in the form of a graph, enabling the observation of cluster separation in the multi-axes space defined by MEF (Multi-Exponential Fit) values. In the first case, the red cluster represents a normal liver, while the green cluster represents metastatic liver. In the second case, the red cluster represents a normal liver, while the green cluster represents abscess liver. In the third case, the red cluster represents abscess liver, and the green cluster represents metastatic liver. Finally, all classes are compared, and the results are displayed as clusters, where the red cluster represents a normal liver, the green cluster represents abscess liver, and the blue cluster represents metastatic liver. This analysis demonstrates that MaZda's texture analysis can

differentiate between normal and diseased liver, as well as distinguish between primary and metastatic liver.

Normalization	Comparison between	Classification rate		
		PCA	LDA	NDA
$\mu \pm 3\sigma$	Abscess and normal	100%	100%	100%
	Metastatic and normal	100%	100%	100%
	Abscess and Metastatic	94.03%	94.03%	94.53%
	Abscess, Metastatic and normal	100%	100%	100%

Table 1: Comparison of performances between different classes of liver diseases and with normal liver using different classification approaches

According to the data presented in the table 1, our system achieves a 100% performance in PCA, LDA, and NDA analyses when comparing abscess and normal liver, as well as metastatic and normal liver and when we have compared all classes (normal, abscess and metastasis). However, when comparing abscess and metastatic liver, our system achieves a performance of 94.03% for PCA and LDA but shows 94.53% classification rate for NDA. Results lower than 100% in the comparison of different diseased liver CT images can be attributed to inter and intra-class variations, errors in marking ROIs leading to the selection of normal tissues along with diseased tissues, and the impact of feature selection and standardization approaches on discrimination performance[2].

The genetic background plays a significant role in the development of liver diseases[21]. In a comparative study, a stochastic gradient descent-based solver was introduced for the purpose of classifying liver diseases [22]. Another study focused on a technique for classifying ultrasonic images of both normal individuals and cirrhotic patients. They tested data parameters through a neural network classifier with scanning dimensions of 64×64[23]. . In a different investigation, researchers worked on combing the conventional statistics and machine learning tools with the convolutional neural network (CNN) to extract features from CT images. They utilized the composite hybrid feature selection (CHFS) system and achieved an accuracy of 96.07%, outperforming the CNN accuracy of 94.11%[24]. %. Furthermore, a study presented a classification rate of approximately 95% for fatty and cirrhosis livers. They used a probabilistic neural network (PNN) classifier which resulted in a sensitivity of 96% and specificity of 94%[25]. %. On study employed an optimal binary logistic regression model for diagnosing Hepatocellular Carcinoma and achieved an accuracy of 84.5%, sensitivity of 84.1% and specificity of 84.9% [26].

Another study proposed a comparative analysis for classifying liver lesions into malignant and benign categories. The ultimate accuracy obtained using positron emission tomography (PET)/CT, magnetic resonance imaging (MRI), and fusion of PET/CT and MRI was 66.7%, 80.0%, and 94.7%, respectively[27]. Additionally, in a study involving 71 patients 312 image samples were analyzed. The study conducted a comparative analysis of 4 classes (abscess, metastatic disease, tumour necrosis, and vascular disorders). Using PCA, LDA, and NDA classifications the results shown high accuracy exceeding 97.86%[23]. With the advancement and in-depth study of Radiomics, medical imaging has extensively explored various disorders in recent years. Textural analysis, a subfield of Radiomics, has emerged as a prominent research area in medical imaging.[17].

4. Conclusion

This study is focuses on liver diseases due to the significance of the liver as a major organ in human body, coupled with the rapid spread of liver diseases. Specifically, medical images obtained from computer tomography scan are utilized to segment and classify different types of human liver diseases using a suitable classifier. The MaZda software serves as a machine learning which

successfully separates these diseases into distinct clusters; clearly differentiating them from both each other and from individuals with normal liver functions.

MaZda software proves to be the valuable tool for discriminating between primary and metastatic liver diseases. Texture analysis tools may help radiologists and doctors to distinguish and diagnose the abnormalities present in the human liver and predict the extent of liver's problems. As this study exclusively focuses on neurons and learning variables, it is essential to investigate the performance of the CAD system concerning other architectural factors, including backpropagation iterations and optimization iterations.

References

1. Krishna, M., *Microscopic anatomy of the liver*. Clinical liver disease, 2013. **2**(Suppl 1): p. S4.
2. Kermani, M.Z. and A. Gharbali, *Automated differentiation of benign and malignant liver tumors by Ultrasound Images*. The Journal of Urmia University of Medical Sciences, 2018. **29**: p. 7.
3. Abdel-Misih, S.R. and M. Bloomston, *Liver anatomy*. Surgical Clinics, 2010. **90**(4): p. 643-653.
4. López-Luque, J. and I. Fabregat, *Revisiting the liver: from development to regeneration-what we ought to know!* International Journal of Developmental Biology, 2018. **62**(6-7-8): p. 441-451.
5. Qian, H., et al., *Autophagy in liver diseases: A review*. Molecular aspects of medicine, 2021. **82**: p. 100973.
6. Ramana, B.V., M.S.P. Babu, and N. Venkateswarlu, *A critical study of selected classification algorithms for liver disease diagnosis*. International Journal of Database Management Systems, 2011. **3**(2): p. 101-114.
7. Cheng, K.-C., et al., *Association of different types of liver disease with demographic and clinical factors*. Biomedicine, 2016. **6**(3): p. 1-7.
8. Gunasundari, S. and S. Janakiraman, *A study of textural analysis methods for the diagnosis of liver diseases from abdominal computed tomography*. International Journal of Computer Applications, 2013. **74**(11).
9. Gharbali, A., *The Application of Texture Analysis for the Study of Liver Disease by Magnetic Resonance Imaging*. 2007, University of Dundee.
10. Yue, Y., et al., *Three-dimensional CT texture analysis to differentiate colorectal signet-ring cell carcinoma and adenocarcinoma*. Cancer Management and Research, 2019. **11**: p. 10445.
11. Summers, R.M., *Texture analysis in radiology: does the emperor have no clothes?* Abdominal Radiology, 2017. **42**(2): p. 342-345.
12. Buch, K., et al., *Using texture analysis to determine human papillomavirus status of oropharyngeal squamous cell carcinomas on CT*. American Journal of Neuroradiology, 2015. **36**(7): p. 1343-1348.
13. Huang, Z., et al., *Two-dimensional texture analysis based on CT images to differentiate pancreatic lymphoma and pancreatic adenocarcinoma: a preliminary study*. Academic radiology, 2019. **26**(8): p. e189-e195.
14. Saleh, A. and R. Lerski, *Texture Discrimination Analysis between Tumour and Healthy Brain Tissue Using MaZda Program*. Al-Nahrain Journal of Science, 2011. **14**(4): p. 57-65.
15. Țălu, Ș., *Texture analysis methods for the characterisation of biological and medical images*. Extreme Life, Biospeology and Astrobiology, 2012. **4**(1): p. 8-12.
16. Nisa, M., et al., *Machine vision-based Statistical texture analysis techniques for characterization of liver tissues using CT images*. 2022. **72**(9): p. 1760-1765.
17. Li, Y., et al., *CT image-based texture analysis to predict microvascular invasion in primary hepatocellular carcinoma*. Journal of Digital Imaging, 2020. **33**: p. 1365-1375.
18. Strzelecki, M., P. Szczypinski, A. Materka, and A. Klepaczko, *A software tool for automatic classification and segmentation of 2D/3D medical images*. Nuclear instruments and methods in physics research section A: Accelerators, Spectrometers, Detectors and associated equipment, 2013. **702**: p. 137-140.
19. Gong, X., et al., *Noninvasive assessment of significant liver fibrosis in rabbits by spectral CT parameters and texture analysis*. Japanese Journal of Radiology, 2023: p. 1-11.

20. Nisa, M., S.A. Buzdar, K. Khan, and M.S. Ahmad, *Deep convolutional neural network based analysis of liver tissues using computed tomography images*. *Symmetry*, 2022. **14**(2): p. 383.
21. Medrano, L.M., M.A. Jiménez-Sousa, A. Fernández-Rodríguez, and S. Resino, *Genetic Polymorphisms Associated with Liver Disease Progression in HIV/HCV-Coinfected Patients*. *AIDS reviews*, 2017. **19**(1): p. 3-15.
22. Hamid, K., A. Asif, W. Abbasi, and D. Sabih. *Machine learning with abstention for automated liver disease diagnosis*. in *2017 International Conference on Frontiers of Information Technology (FIT)*. 2017. IEEE.
23. Nisa, M., et al., *Machine vision-based Statistical texture analysis techniques for characterization of liver tissues using CT images*. *JPMA. The Journal of the Pakistan Medical Association*, 2022. **72**(9): p. 1760-1765.
24. Kumar, P., R. Kumar, and M.V. Reddy, *Assessment of sewage treatment plant effluent and its impact on the surface water and sediment quality of river Ganga at Kanpur*. *Int J Sci Eng Res*, 2017. **8**(1): p. 1315-1324.
25. Mala, K., V. Sadasivam, and S. Alagappan, *Neural network based texture analysis of CT images for fatty and cirrhosis liver classification*. *Applied Soft Computing*, 2015. **32**: p. 80-86.
26. Stocker, D., et al., *MRI texture analysis for differentiation of malignant and benign hepatocellular tumors in the non-cirrhotic liver*. *Heliyon*, 2018. **4**(11): p. e00987.
27. Waite, S., et al., *Communication errors in radiology—Pitfalls and how to avoid them*. *Clinical Imaging*, 2018. **51**: p. 266-272.